RSC Advances

PAPER

View Article Online
View Journal | View Issue

Cite this: *RSC Adv.*, 2019, **9**, 8759

Synthesis and characterization of ethyl benzotriazolyl acrylate-based D–π–A fluorophores for live cell-based imaging applications†

Ana Sofia Ortega-Villarreal,[a] Eugenio Hernández-Fernández,*[a] Christopher Jensen,[b] Gabriel A. Valdivia-Berroeta,[b] Samuel Garrard,[b] Israel López,[ac] Stacey J. Smith,[b] Kenneth A. Christensen,[b] Miguel A. Reyes-González[a] and David J. Michaelis*[b]

Received 5th January 2019
Accepted 5th March 2019

DOI: 10.1039/c9ra00108e

rsc.li/rsc-advances

A series of eight new ethyl (*Z*)-benzotriazolyl acrylates **6a–d** and **7a–d** have been synthesized by conventional heating and microwave irradiation from ethyl benzotriazolyl acetates **3** and **4** with the corresponding aromatic aldehydes. This work reports the synthetic approach and spectroscopic characterization (^{1}H, ^{13}C-NMR, HRMS) of all the synthesized compounds. X-ray diffraction analyses were performed for molecules **6a**, **7a** and **7d**. Photophysical properties of compounds were evaluated. Finally, compound **6a** was tested in a human cell line and showed low to no cytotoxicity at relevant concentrations. Initial testing demonstrates its potential use as a fluid-phase fluorescent marker for live cell imaging.

Introduction

Organic fluorescent molecules have gained great attention in recent decades due to their diverse applications both in chemistry [organic light-emitting diodes (OLED),[1–3] organic photovoltaic devices (OPV),[4,5] organic field-effect transistors (OFET),[6,7] organic thin film transistors (OTFT), metal ion sensors[8]] and in biology (fluorescent tags,[9,10] pH monitoring in biological systems,[11] biological species sensors[12,13] and cell bioimaging[9,14–16]). The possibility of using this class of fluorescent compounds for these applications is related to their chemical (reactivity, solubility, lipophilicity and stability) and photophysical properties [excitation maximum (λ_{ex}), emission maximum (λ_{em}), extinction coefficient (ε), quantum yield (ϕ), lifetime of the excited state and photostability].[17,18]

The design and synthesis of fluorescent molecules requires incorporating certain structural characteristics that include multiple combined aromatic groups, planar or cyclic molecules with several π bonds, conjugated double bonds, and resonance.[19] α,β-Unsaturated carbonyl compounds and benzotriazoles are examples of structural motifs that could be promising fluorophores and which are of particular interest in our research groups. Benzotriazole derivatives are well-known for their biological applications,[20–22] including their use as antibacterial,[23] antitubercular,[24] antifungal,[25] antiviral,[26] anti-inflammatory,[27] anticonvulsant,[28] and anticancer[29] agents. In addition, the extended conjugated system in benzotriazoles makes them promising candidates for biological probes that exhibit fluorescence.[30,31] Thus, our goal from the outset was to explore how the biocompatible structure of the benzotriazole could be combined with their fluorescent properties to construct fluorescence probes capable of measuring a variety of biological processes.

Preparation of α,β-unsaturated carbonyls can be achieved through several conventional routes including aldol condensation, carbon halogenation followed by elimination, oxidation of allylic alcohols and Wittig reactions, among others.[32] An alternative route to synthesize these compounds is the Doebner modification[33] of the Knoevenagel condensation,[34] which can be carried out in the presence of carboxylic acid functional groups. Nevertheless, preparation of α,β-unsaturated esters incorporating a benzotriazole group in the α position has not been reported and this approach could afford a practical and useful series of new compounds with enhanced fluorescent properties. Herein, we report the synthesis of eight ethyl benzotriazolyl

[a]*Universidad Autónoma de Nuevo León, Facultad de Ciencias Químicas, Pedro de Alba s/n, Ciudad Universitaria, 66400, San Nicolás de los Garza, Nuevo León, Mexico. E-mail: eugenio.hernandezfr@uanl.edu.mx; Fax: +52 81 1340 4890 ext. 6293; Tel: +52 81 1340 4890 ext. 6293*

[b]*Department of Chemistry and Biochemistry, Brigham Young University, 84602, Provo, Utah, USA. E-mail: dmichaelis@chem.byu.edu; Tel: +1 801 422 9416*

[c]*Universidad Autónoma de Nuevo León, UANL, Centro de Investigación en Biotecnología y Nanotecnología (CIBYN), Laboratorio de Nanociencias y Nanotecnología, Autopista al Aeropuerto Internacional Mariano Escobedo Km. 10, Parque de Investigación e Innovación Tecnológica (PIIT), 66629 Apodaca, Nuevo León, Mexico*

† Electronic supplementary information (ESI) available. CCDC 1882468, 1867840 and 1882467. For ESI and crystallographic data in CIF or other electronic format see DOI: 10.1039/c9ra00108e

acrylates using conventional heating and microwave irradiation techniques. Additionally, the crystallographic and photophysical properties of these new compounds are reported. Cytotoxicity, cell labeling and localization of one of the compounds are tested.

Results and discussion

Synthesis of ethyl benzotriazolyl acrylates 6a–d and 7a–d

For the synthesis of target compounds **6a–d** and **7a–d**, benzotriazole was reacted with ethyl bromoacetate and K_2CO_3 as a base to obtain precursors **3** and **4** (Scheme 1). In this reaction, both the 1*H* and 2*H*-isomers of benzotriazole were obtained due to the inherent tautomeric structure of benzotriazole.[20,35] In our synthesis, the 1*H*-isomer was obtained in greater yield (86% compared to 12% yield). These results agree with chemical evidence supported by ultraviolet, infrared and proton nuclear magnetic resonance spectra studies indicating the predominance of the 1*H*-isomer at room temperature.[36–38] In addition, the large dipole moment of the 1*H*-tautomer enhances its stability over the 2*H*-isomer because of the different intermolecular interactions taking place either with itself (in the solid state) or with the solvent (in solution).[35]

Compounds **3** and **4** served as common intermediates for the preparation of all our acrylate derivatives *via* condensation with commercially available aromatic aldehydes. The α,β-unsaturated acrylates **6a–d** and **7a–d** were synthesized by Knoevenagel condensation reaction between **3** and **4** and a variety of aromatic aldehydes, including 4-(dimethylamino)benzaldehyde, 4-(diethylamino)benzaldehyde, 4-(diphenyl-amino) benzaldehyde and 4-(4-morpholinyl)benzaldehyde (**5a–d**). This condensation reaction was conducted using piperidine as the stoichiometric base and ethanol as solvent (Table 1).

Our results in Table 1 demonstrate that the reaction of compound **3** with aromatic aldehydes **5a–d** afforded ethyl benzotriazolyl acrylates **6a–d** with yields ranging from 20% to 87% under reflux conditions. Good yields were obtained for compounds **6a**, **6b** and **6d**. However, compound **6c** was obtained with a 20% yield. We suspected that the low yield could be strongly influenced by the lower reactivity of the 4-(diphenylamino)benzaldehyde; therefore, we decided to carry out the reaction under microwave irradiation, in accordance with our previous studies.[39,40] We found that at 100 °C for 80 min, the yield of **6c** increased from 20% to 56%. The reaction of benzotriazole **4** with aromatic aldehydes **5a** and **5d** afforded ethyl benzotriazolyl acrylates **7a** and **7d** with yields of 61% and 71%. In a similar way, we performed the microwave irradiation reaction for compounds **7b** and **7c** and we were able to increase the yields from 10% and 2% up to 75% and 50%, respectively.

Single-crystal X-ray diffraction analyses

Based on the crystal structures of **6a**, **7a** and **7d**, the (*Z*)-geometry of the double-bond was unequivocally confirmed (Fig. 1). The angle between the benzene and benzotriazole rings in each structure was calculated using the non-hydrogen atoms to define planes containing each ring; the angles between these planes were found to be 87.7°, 72.6° and 76.9°, respectively. This near perpendicular orientation is likely due to steric hindrance between the aromatic rings. Details of the crystal structure of **6a**, **7a** and **7d** derivatives are listed in Table 2.

Photophysical properties

The photophysical properties of compounds **6a–d** and **7a–d** were analyzed in solution, at 10^{-5} M, using methanol as solvent. Fig. 2 shows the absorption bands of these compounds, which are located between 300 and 450 nm, and are attributed to n–π* transitions; absorbance data were normalized. The wavelengths of maximum absorption, λ_{Abs}, for each derivative in both symmetrical and asymmetrical isomers are the same. Compounds **6b-c** and **7b-c** presented an equal value of λ_{Abs}, and compounds **6b** and **6c** also showed the same absorption pattern between 340 and 460 nm. However, **6b** uniquely presents a second absorption band at 271 nm, which could be attributed to a second chromophore, but we did not record an emission spectrum due to its short value (<400 nm) (Fig. S20, ESI†). Table 3 shows the λ_{Abs} values for each compound and their corresponding photon energy, E_{Abs}. Similar to the behavior of λ_{Abs}, the extinction coefficient, ε, for each derivative in both isomeric series are of comparable magnitude and presented high values (>30 000 M^{-1} cm^{-1}), making them suitable for biological and medical applications.[41]

The first excitation wavelength probed for each compound was λ_{Abs}, then the wavelength of maximum emission, λ_{Em}, was fixed and the excitation spectra were collected. After that, the maximum of the excitation spectra, λ_{Ex}, was fixed as corrected excitation wavelength, only in the case of **6b** derivative, the λ_{Em} was shifted after this correction. The emission spectra collected with the corrected excitation wavelength are shown in Fig. 3. The emission pattern of **6b** and **6c** derivatives is the same, which was expected due to observations in the UV-vis spectra. The UV spectra indicates that the excitation and emission processes for both molecules possess the same energy levels. Therefore, we can conclude that their non-radiative processes are equivalent.[42]

The Stokes shift, SS, is the difference between the absorption and emission maxima,[43] and is indicated in the following equation:

$$SS = \lambda_{Em} - \lambda_{Abs} \quad (1)$$

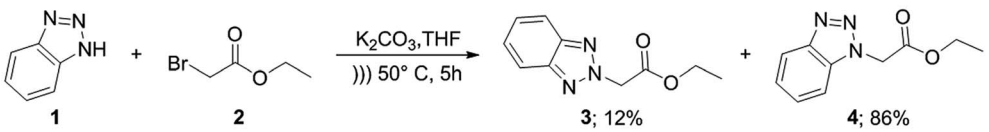

Scheme 1 Synthesis of ethyl benzotriazolyl acetates **3** and **4**.

Table 1 Synthesis of ethyl benzotriazolyl acrylates **6a–d** and **7a–d**

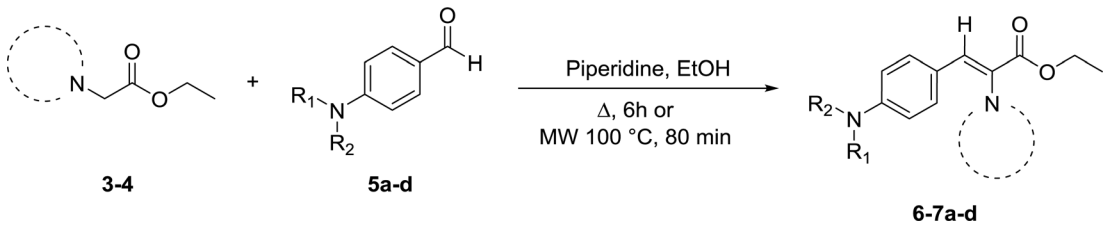

3-4 **5a-d** **6-7a-d**

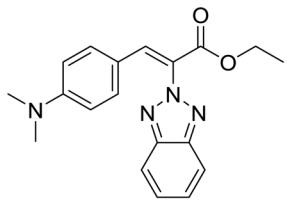

6a;
87%[a]

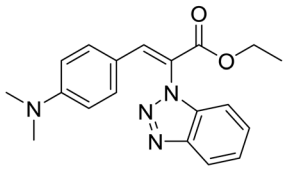

7a;
61%[a]

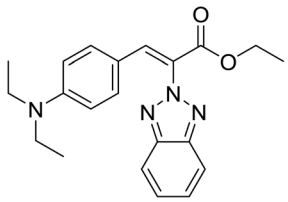

6b;
72%[a]

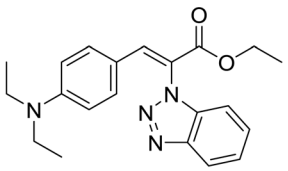

7b;
10%[a]
75%[b]

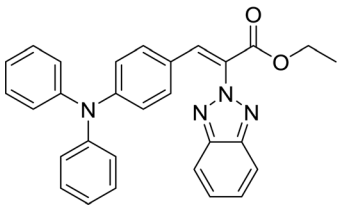

6c;
20%[a]
56%[b]

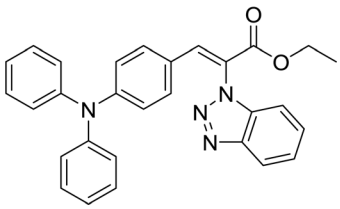

7c;
2%[a]
50%[b]

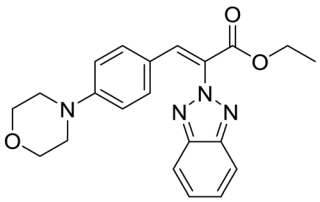

6d;
71%[a]

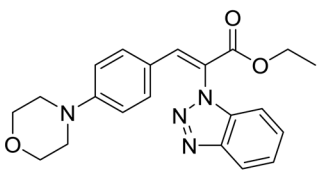

7d;
71%[a]

[a] Conventional heating. [b] Microwave irradiation.

A large SS is one important property that should be considered when identifying potentially useful fluorescent markers or labels for cell-based analysis. Table 3 shows the SS values in nm for derivatives **6** and **7**, and their equivalence in eV. In contrast with the other photophysical parameters previously mentioned, the SS value does not appear to follow a trend that depends on the substituent on the aromatic aldehyde or on the substitution of the benzotriazole ring. From these studies, we selected

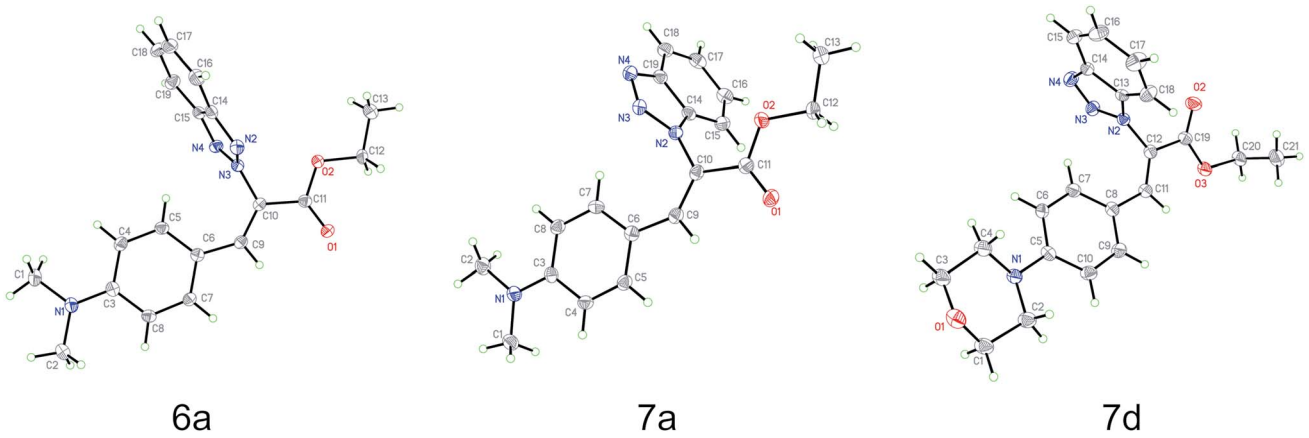

Fig. 1 Molecule structures of ethyl benzotriazolyl acrylates **6a** (CCDC 1882468), **7a** (CCDC 1867840) and **7d** (CCDC 1882467) determined by single-crystal X-ray diffraction analysis.

Table 2 Crystallographic data and refinement metrics for **6a**, **7a** and **7d**

Compound	**6a**	**7a**	**7d**
Chemical formula	$C_{19}H_{20}N_4O_2$	$C_{19}H_{20}N_4O_2$	$C_{21}H_{22}N_4O_3$
M	336.39 g mol^{-1}	336.39 g mol^{-1}	378.42 g mol^{-1}
Crystal system	Monoclinic	Monoclinic	Orthorhombic
Space group	$P2_1/c$	$P2_1/c$	$Pca2_1$
a	9.0183(7) Å	13.2422(7) Å	17.5573(10) Å
b	8.3790(7) Å	8.7080(5) Å	6.3237(4) Å
c	23.0425(18) Å	29.4352(16) Å	33.7271(19) Å
α	90°	90°	90°
β	97.233(4)°	96.420(3)°	90°
γ	90°	90°	90°
V	1727.3(2) Å^3	3373.0(3) Å^3	3744.6(4) Å^3
R_1	0.0366	0.0369	0.0362
wR_2	0.0943	0.0944	0.0958

derivative **6a** for further photophysical and biological testing due to the combination of its features: high chemical yield, visible λ_{Abs}, high ε, and large SS.

Fig. 4 shows the absorption and emission spectra of the **6a** derivative depicting its large SS (128 nm) like other commonly used fluorophores with similar properties (*e.g.* Lucifer yellow, Pacific orange) that are used in fluorescence microscopy and flow cytometry. Compound **6a** was tested as fluorescent label for mammalian cells. An additional experiment using a DMSO stock solution (needed for cell-based assays) was performed in order to confirm that its photophysical properties were not significantly modified (Fig. S21, ESI†).

In vitro cytotoxicity and cell imaging

The cytotoxicity of the selected derivative **6a** was assessed following a 24 h treatment to the cells by measuring conversion of resazurin to resorufin, a common indicator of cell viability, over a 4 h period. The results showed limited cytotoxicity of compound **6a** for HEK 293T cells (a human cell line) even at concentrations of 50 μM that are about 5× greater than would typically be used. At this concentration, cell viability was reduced to only 64 ± 4% compared to the vehicle control (Fig. 5).

Based on this data, compound **6a** appears to be similarly or less toxic than other commonly-used fluorophores such as Rhodamine 6G and Cy5.5 indicating its potential for use as

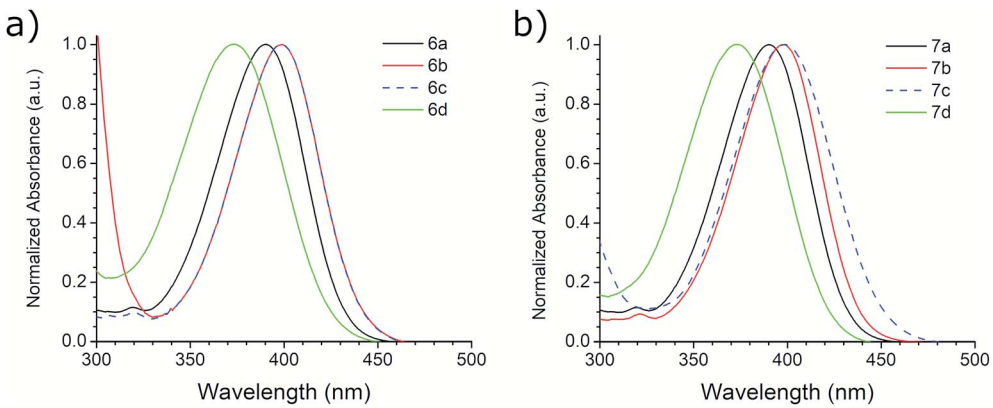

Fig. 2 Absorption spectra of (a) **6a–d** and (b) **7a–d** ethyl benzotriazolyl acrylate derivatives.

Table 3 Photophysical properties of **6** and **7** derivatives in methanol

Compound	λ_{Abs} (nm)	E_{Abs} (eV)	ε (10^4 M^{-1} cm^{-1})	λ_{Em} (λ_{Ex}) (nm)	E_{em} (eV)	SS (nm)	SS (eV)
6a	391	3.17	3.28	519 (416)	2.39	128	0.78
6b	399	3.11	3.32	463 (363)	2.68	64	0.43
6c	398	3.12	4.26	463 (363)	2.68	65	0.44
6d	372	3.33	2.79	505 (340)	2.46	133	0.88
7a	390	3.18	3.27	467 (413)	2.66	77	0.52
7b	398	3.12	3.37	466 (398)	2.66	68	0.45
7c	398	3.12	4.26	566 (395)	2.19	168	0.92
7d	372	3.33	2.79	467 (393)	2.66	95	0.68

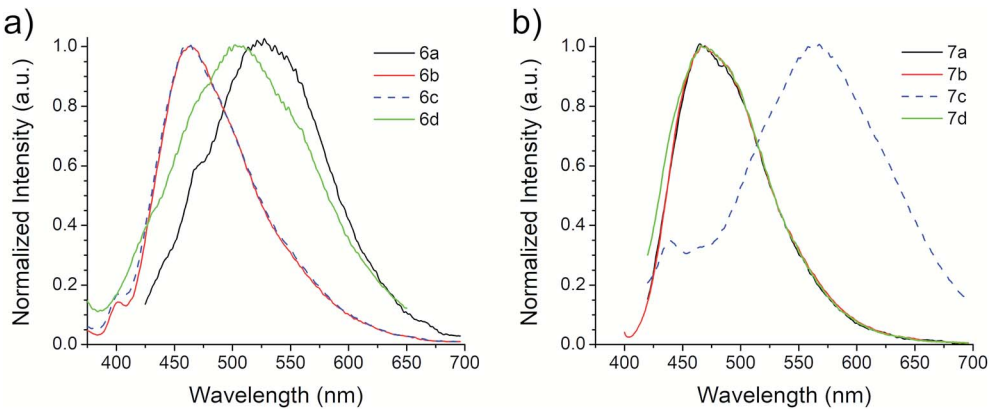

Fig. 3 Emission spectra of (a) **6a–d** and (b) **7a–d** ethyl benzotriazolyl acrylate derivatives.

a marker for *in vitro* and *ex vivo* cell studies.[44] Additionally, compound **6a** exhibits a unique absorption–emission profile compared to many other mammalian cell-safe fluorophores,[45] which may further promote its utility in these types of assays.

Derivative **6a** was also analyzed *via* confocal microscopy for cellular staining, uptake and localization in HEK 293T cells. Many fluorescent molecules and nanoparticles are largely internalized by cells *via* endocytosis. To determine localization of **6a**, cells were co-incubated with 50 μg mL^{-1} of Dextran–Cascade Blue, DCB, a fluorescent conjugate which localizes to endosomes[46] and eventually fuses with lysosomes.[47] Confocal analysis of cells revealed that derivative **6a** accumulated in vesicle-like structures located in the cytosol, often co-localizing with DCB (Fig. 6a). This suggests that **6a** is localized to endosomes and/or lysosomes when taken up by the cell. Additionally, a modified experiment performed by removing DCB after 4 h prior to imaging showed broad co-localization of the two fluorophores once again, indicating that **6a** is indeed trafficked along the endocytic pathway to late endosomes and lysosomes (Fig. 6b). Based on these results, it appears that the cellular localization and fates of **6a** and dextrans are similar making **6a** a fluid-phase probe similar to conjugated dextrans. It is anticipated modifications could be made to the compound to change the mechanism of uptake and localization in cells without disrupting the fluorophore. In addition, small molecular weight fluorescent compounds, like those described here, are uniquely suited as minimally perturbing labels for larger biomolecules and even metabolites for use in cell-based assays and imaging.

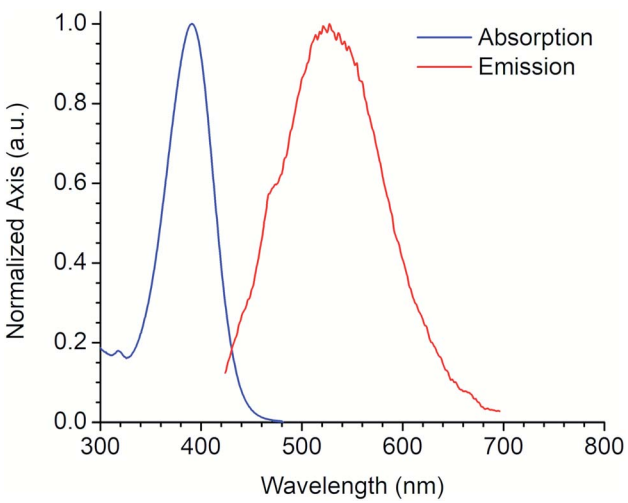

Fig. 4 Absorption and emission spectra of **6a** derivative.

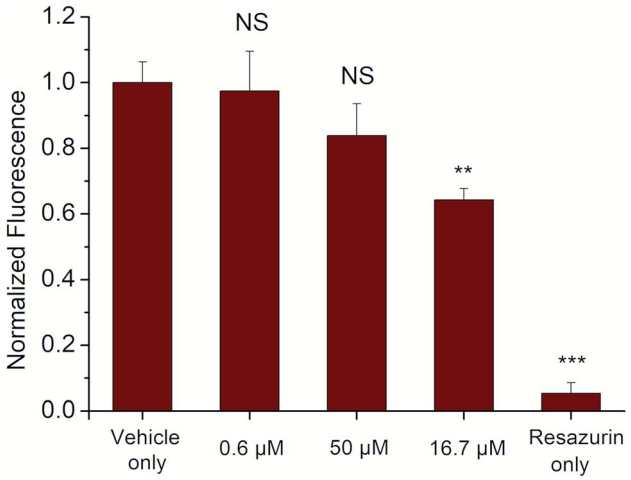

Fig. 5 Cell toxicity of compound **6a** at various concentrations. After 24 h incubation with derivative **6a** at 50 μM, cells retained 64 ± 4% viability compared to control cells. Incubation with 0.6 μM **6a** appeared to have negligible cytotoxicity. Significance was assessed relative to positive control using a two-tailed *t* test (NS: no significance, $^{**}P < 0.01$, $^{***}P < 0.001$).

Conclusions

In this work, we present eight ethyl benzotriazolyl acrylate derivatives prepared using the Knoevenagel condensation reaction with yields from 50% to 87%. In general, the synthesis was efficient using conventional heating methods, yet the yields improved when compounds **6c**, **7b** and **7c** were synthesized under microwave irradiation conditions. The (*Z*)-geometry of double-bond was confirmed for compounds **6a**, **7a** and **7d** by single-crystal X-ray diffraction. The optical properties assay showed that compounds **6a**, **6d** and **7c** presented a wider Stoke shift, therefore, derivative **6a** was employed to evaluate its toxicity and to generate bioimages. Finally, based on the relatively mild toxicity, broad Stokes shift, and definitive cellular localization data collected for **6a**, we have demonstrated the potential of this kind of molecules to serve as a novel cell-safe fluorophore that can be used in a variety of assays.

Experimental

Materials and instruments

All commercial materials were used as received unless noted otherwise. Melting points were registered using an Electrothermal Mel-Temp apparatus and are uncorrected. Thin-layer chromatography was performed on pre-coated sheets of silica

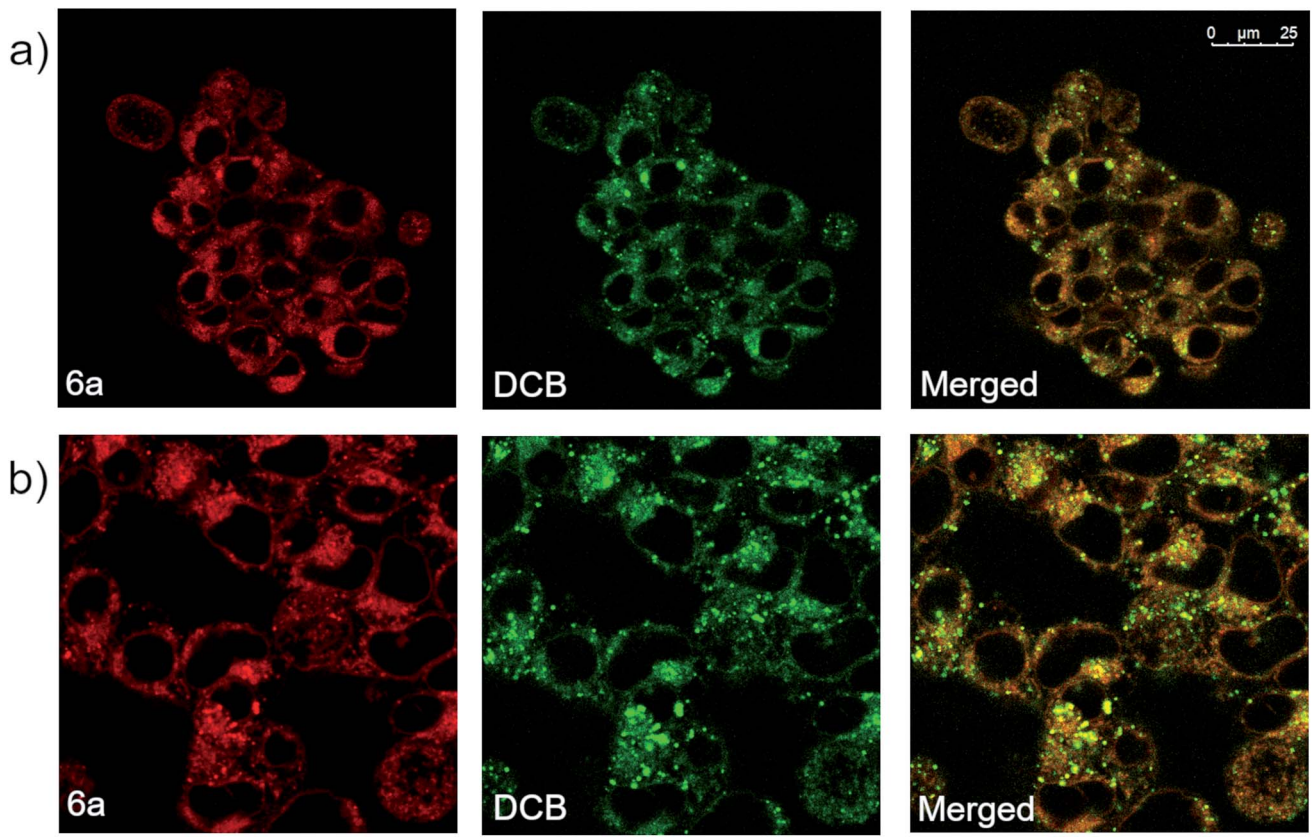

Fig. 6 (a) Confocal fluorescence microscopic images of HEK 293T cells incubated with derivative **6a** (10 μM) and DCB (50 μg mL^{-1}) for 16 h, and (b) confocal fluorescence microscopic images of modified assay in which HEK 293T cells were incubated with **6a** (10 μM) and DCB (50 μM) for 20 h, then **6a** (10 μM) alone for 4 h.

gel 60 F254 (E. Merck). For column chromatography 230–400 mesh silica gel 60 (E. Merck) was used as stationary phase. The spectra were obtained in $CDCl_3$ solution using TMS as the internal reference. ^{1}H NMR data were acquired on an Inova 300 MHz, an Inova 500 MHz, or an NMR-S 500 MHz spectrometer. Chemical shifts (δ) are reported in parts per million and coupling constants were expressed as (J) and reported in Hertz (Hz). Multiplicities are reported as follows: s (singlet), d (doublet), t (triplet), q (quartet), m (multiplet). ^{13}C NMR data were acquired on an Inova at 75 MHz or Inova NMR-S spectrometer at 125 MHz. Mass spectral data were obtained using ESI techniques (Agilent, 6210 TOF). Reactions carried out with stirring under microwave irradiation in closed-vessels were all performed with a CEM Discover Synthesizer. For the photophysical characterization reagent-grade methanol was used as solvent. UV-vis absorption spectra were recorded on a Shimadzu 1800 spectrophotometer using quartz cuvettes (1 cm path length). Emission spectra were measured on a Perkin-Elmer LS 55 fluorescence spectrophotometer using quartz cuvettes (1 cm path length). For *in vitro* cytotoxicity and confocal microscopy assays, HEK 293T cells (ATCC) were cultured at 37 °C and 5% CO_2 in Dulbecco's Modified Eagle Medium (GenClone) supplemented with 10% fetal bovine serum (VWR). For cell-based assays, cells were trypsinized with 0.25% trypsin solution in HBSS (GenClone) and seeded in 96-well optical plate (Nunc). Resazurin solution was prepared by dissolving powered resazurin (Acros) in phosphate buffered saline (Thermo Fisher) to a final concentration of 100 μg mL^{-1}. Solutions of **6a** were prepared by adding lyophilized **6a** to pure DMSO (EMD Millipore) to a final concentration of 1 mg mL^{-1}. Sample fluorescence was measured using a Synergy H4 Hybrid plate reader (BioTek). DCB was obtained from Thermo Fisher. Confocal microscopy was performed with a Leica DMi8 confocal microscope. Image analysis was performed in the LAS X Life Science platform (Leica Microsystems).

Procedure for the synthesis of ethyl benzotriazolyl acetates 3 and 4

To a suspension of benzotriazole **1** (1 equiv.), ethyl bromoacetate **2** (1.2 equiv.) and K_2CO_3 (1.5 equiv.) in THF was sonicated at 50 °C for 5 h. Solvent was then evaporated under reduced pressure and water was added. The mixture was extracted with EtOAc. The combined organic extracts were dried over anhydrous Na_2SO_4, filtered and concentrated under reduced pressure. The solid obtained was purified by column chromatography on silica gel using *n*-hexane/EtOAc (3 : 1) as eluent to obtain both isomers **3** and **4**.

Ethyl 2-(2*H*-benzotriazol-2-yl)acetate 3. (12%) White solid, mp 122–124 °C; ^{1}H NMR (500 MHz, $CDCl_3$): δ 1.27 (t, J = 7.1 Hz, 3H), 4.27 (q, J = 7.1 Hz, 2H), 5.53 (s, 2H), 7.38–7.42 (m, 2H), 7.86–7.90 (m, 2H); ^{13}C NMR (125 MHz, $CDCl_3$): δ 14.1, 57.2, 62.5, 118.3, 127.0, 145.0, 166.3. HRMS (ESI$^+$) m/z calcd for $C_{10}H_{12}N_3O_2$ [M + H]$^+$ 206.09295, found 206.09214 (literature 48).

Ethyl 2-(1*H*-benzotriazol-1-yl)acetate 4. (86%) White solid, mp 83–84 °C; ^{1}H NMR (500 MHz, $CDCl_3$): δ 1.26 (t, J = 7.1 Hz, 3H), 4.25 (q, J = 7.1 Hz, 2H), 5.42 (s, 2H), 7.38–7.53 (m, 3H), 8.08 (d, J = 8.4 Hz, 1H); ^{13}C NMR (125 MHz, $CDCl_3$): δ 14.1, 49.1, 62.3, 109.2, 120.2, 124.1, 127.9, 133.4, 146.0, 166.4. HRMS (ESI$^+$) m/z calcd for $C_{10}H_{12}N_3O_2$ [M + H]$^+$ 206.09295, found 206.09223 (literature 48).

General procedure for the synthesis of ethyl benzotriazolyl acrylates 6a–d and 7a–d

A solution of the corresponding ethyl benzotriazolyl acetate (**3**, **4**) (1 equiv.), appropriate aromatic aldehydes **5a–d** (1 equiv.) and piperidine (2 equiv.) in ethanol (20 mL) was reacted under reflux by conventional heating for 6 h. Solvent was evaporated under reduced pressure. The crude was purified either by column chromatography on silica gel using pure hexane to 70% hexane/EtOAc as eluent or by crystallization under ethanol. The final products were characterized by ^{1}H and ^{13}C NMR spectroscopy and HRMS. ^{1}H and ^{13}C-NMR spectra can be found in ESI (Fig. S1–S16†).

Procedure for the synthesis of ethyl benzotriazolyl acrylates 6c, 7b and 7c using microwave irradiation

In a capped 10 mL MW vessel, the corresponding ethyl benzotriazolyl acetate (**3**, **4**) (1 equiv.), appropriate aromatic aldehydes **5b-c** (1 equiv.), piperidine (2 equiv.) and ethanol (4 mL) were mixed. The tube was positioned in the irradiation cavity and the mixture was heated with stirring under microwave irradiation at 100 °C and held for 80 min. The vessel was cooled to room temperature and the residue was dissolved in methanol and then concentrated under reduced pressure. The crude was purified either by column chromatography on silica gel using pure hexane to 70% hexane/EtOAc as eluent or by crystallization under ethanol.

Ethyl (*Z*)-2-(2*H*-benzotriazol-2-yl)-3-(4(dimethylamino)phenyl) acrylate 6a. Yellow solid, mp 160–162 °C; ^{1}H NMR (300 MHz, $CDCl_3$): δ 1.24 (t, J = 7.1 Hz, 3H), 2.92 (s, 6H), 4.27 (q, J = 7.1 Hz, 2H), 6.37 (d, J = 9.2 Hz, 2H), 6.44 (d, J = 9.2 Hz, 2H), 7.42–7.49 (m, 2H), 7.94–8.00 (m, 2H), 8.01 (s, 1H); ^{13}C NMR (75 MHz, $CDCl_3$): δ 14.2, 39.8, 61.6, 111.5, 118.0, 118.8, 123.9, 126.8, 132.8, 141.1, 145.0, 152.2, 163.9. HRMS (ESI$^+$) m/z calcd for $C_{19}H_{21}N_4O_2$ [M + H]$^+$ 337.16645, found 337.16666.

Ethyl (*Z*)-2-(2*H*-benzotriazol-2-yl)-3-(4-(diethylamino)phenyl) acrylate 6b. Yellow solid, mp 142–144 °C; ^{1}H NMR (300 MHz, $CDCl_3$): δ 1.08 (t, J = 7.1 Hz, 6H), 1.24 (t, J = 7.1 Hz, 3H), 3.28 (q, J = 7.1 Hz, 4H), 4.26 (q, J = 7.1 Hz, 2H), 6.34 (d, J = 9.2 Hz, 2H), 6.41 (d, J = 9.2 Hz, 2H), 7.44–7.48 (m, 2H), 7.96–7.98 (m, 1H), 7.99 (s, 1H); ^{13}C NMR (125 MHz, $CDCl_3$): δ 12.6, 14.4, 44.5, 61.7, 111.2, 117.4, 119.0, 123.4, 126.9, 133.3, 141.2, 145.1, 150.2, 164.2. HRMS (ESI$^+$) m/z calcd for $C_{21}H_{25}N_4O_2$ [M + H]$^+$ 365.19775, found 365.19606.

Ethyl (*Z*)-2-(2*H*-benzotriazol-2-yl)-3-(4-(diphenylamino)phenyl) acrylate 6c. Yellow oil; ^{1}H NMR (300 MHz, $CDCl_3$): δ 1.24 (t, J = 7.1 Hz, 3H), 4.28 (q, J = 7.1 Hz, 2H), 6.40 (d, J = 8.9 Hz, 2H), 6.68 (d, J = 8.9 Hz, 2H), 7.00–7.11 (m, 6H), 7.19–7.29 (m, 4H), 7.36–7.46 (m, 2H), 7.91–7.97 (m, 2H), 8.01 (s, 1H); ^{13}C NMR (75 MHz, $CDCl_3$): δ 14.3, 62.1, 118.3, 118.9, 120.2, 121.6, 122.8, 124.2, 124.8, 125.6, 126.1, 127.3, 129.6, 129.7, 132.3, 140.3, 145.1, 146.3, 151.0,

164.4; HRMS (ESI$^+$) m/z calcd for $C_{29}H_{25}N_4O_2$ $[M + H]^+$ 461.19775, found 461.19840.

Ethyl (*Z*)-2-(2*H*-benzotriazol-2-yl)-3-(4-morpholinophenyl)acrylate 6d. Yellow solid, mp 82–84 °C; ^{1}H NMR (300 MHz, $CDCl_3$): δ 1.25 (t, $J = 7.1$ Hz, 3H), 3.16 (t, $J = 5.1$ Hz, 4H), 3.75 (t, $J = 4.8$ Hz, 4H), 4.28 (q, $J = 7.1$ Hz, 2H), 6.49 (d, $J = 9.1$ Hz, 2H), 6.58 (d, $J = 9.1$ Hz, 2H), 7.40–7.52 (m, 2H), 7.91–8.0 (m, 2H), 8.02 (s, 1H). ^{13}C NMR (75 MHz, $CDCl_3$): δ 14.3, 47.4, 62.0, 66.6, 114.1, 118.9, 121.1, 125.7, 127.2, 132.6, 140.6, 145.1, 153.0, 163.7. HRMS (ESI$^+$) m/z calcd for $C_{21}H_{23}N_4O_3$ $[M + H]^+$ 379.17702, found 379.17717.

Ethyl (*Z*)-2-(1*H*-benzotriazol-1-yl)-3-(4-(dimethylamino)phenyl) acrylate 7a. Yellow solid, mp 152–154 °C; ^{1}H NMR (300 MHz, $CDCl_3$): δ 1.19 (t, $J = 7.1$ Hz, 3H), 2.91 (s, 6H), 4.23 (q, $J = 7.1$ Hz, 2H), 6.36 (d, $J = 9.1$ Hz, 2H), 6.58 (d, $J = 9.1$ Hz, 2H), 7.29–7.48 (m, 3H), 8.11 (s, 1H), 8.15 (d, $J = 7.4$ Hz, 1H); ^{13}C NMR (125 MHz, $CDCl_3$): δ 14.2, 39.8, 61.5, 110.1, 111.5, 117.7, 118.2, 119.9, 124.1, 128.0, 132.8, 133.6, 142.2, 145.8, 152.1, 164.3. HRMS (ESI$^+$) m/z calcd for $C_{19}H_{21}N_4O_2$ $[M + H]^+$ 337.16645, found 337.16540.

Ethyl (*Z*)-2-(1*H*-benzotriazol-1-yl)-3-(4-(diethylamino)phenyl) acrylate 7b. Yellow solid, mp 118–120 °C; ^{1}H NMR (300 MHz, $CDCl_3$): δ 1.07 (t, $J = 7.1$ Hz, 6H), 1.18 (t, $J = 7.1$ Hz, 3H), 3.26 (q, $J = 7.1$ Hz, 4H), 4.22 (q, $J = 7.1$ Hz, 2H), 6.33 (d, $J = 9.1$ Hz, 2H), 6.54 (d, $J = 9.1$ Hz, 2H), 7.31–7.48 (m, 3H), 8.10 (s, 1H), 8.12–8.18 (d, $J = 8.3$ Hz, 1H); ^{13}C NMR (75 MHz, $CDCl_3$): δ 12.5, 14.2, 44.4, 61.5, 110.2, 111.1, 117.0, 117.6, 120.0, 124.1, 128.0, 133.3, 133.7, 142.3, 145.8, 150.1, 164.5. HRMS (ESI$^+$) m/z calcd for $C_{21}H_{25}N_4O_2$ $[M + H]^+$ 365.19775, found 365.19818.

Ethyl (*Z*)-2-(1*H*-benzotriazol-1-yl)-3-(4-(diphenylamino)phenyl) acrylate 7c. Yellow oil; ^{1}H NMR (300 MHz, $CDCl_3$): δ 1.19 (t, $J = 7.1$ Hz, 3H), 4.24 (q, $J = 7.1$ Hz, 2H), 6.53 (d, $J = 8.9$ Hz, 2H), 6.68 (d, $J = 8.9$ Hz, 2H), 6.99–7.11 (m, 6H), 7.19–7.28 (m, 4H), 7.31–7.50 (m, 3H), 8.11 (s, 1H), 8.12 (d, $J = 8.3$ Hz, 1H); ^{13}C NMR (75 MHz, $CDCl_3$): δ 14.3, 61.9, 110.1, 120.0, 120.2, 123.0, 124.2, 124.9, 125.7, 126.1, 128.2, 129.7, 132.2, 133.6, 141.4, 145.8, 146.1, 150.8, 164.0. HRMS (ESI$^+$) m/z calcd for $C_{29}H_{25}N_4O_2$ $[M + H]^+$ 461.19775, found 461.19910.

Ethyl (*Z*)-2-(1*H*-benzotriazol-1-yl)-3-(4-morpholinophenyl)acrylate 7d. Yellow solid, mp 134–136 °C; ^{1}H NMR (500 MHz, $CDCl_3$): δ 1.20 (t, $J = 7.1$ Hz, 3H), 3.16 (t, $J = 5.1$ Hz, 4H), 3.75 (t, $J = 5.1$ Hz, 4H), 4.24 (q, $J = 7.1$ Hz, 2H), 6.57 (d, $J = 9.1$ Hz, 2H), 6.63 (d, $J = 9.1$ Hz, 2H), 7.31 (d, $J = 8.1$ Hz, 1H), 7.38–7.47 (m, 2H), 8.12 (s, 1H), 8.15 (d, $J = 8.4$ Hz, 1H); ^{13}C NMR (125 MHz, $CDCl_3$): δ 14.3, 47.3, 61.9, 66.5, 110.1, 114.0, 119.8, 120.2, 121.3, 124.2, 128.2, 132.7, 133.6, 141.7, 145.9, 152.9, 164.1. HRMS (ESI$^+$) m/z calcd for $C_{21}H_{23}N_4O_3$ $[M + H]^+$ 379.17702, found 379.17870.

Single-crystal X-ray diffraction analyses

Compounds **6a**, **7a**, and **7d** were crystallized using slow evaporation in ethyl acetate/hexanes to afford yellow single crystals for X-ray diffraction experiments. High-resolution (0.84 Å) data were collected at 100 K utilizing Cu K_α radiation produced by a Bruker-Nonius FR591 rotating anode X-ray source coupled to a MACH3 kappa goniometer and Bruker Apex II CCD detector. The Bruker APEX3 software package was utilized to integrate, scale and correct the obtained data. The structure was solved using dual-space methods in SHELXT[49] and refined against F^2 on all data by full-matrix least squares with SHELXL-2014 (ref. 50) using established refinement strategies.[51]

In vitro cytotoxicity and cell imaging

For *in vitro* cell toxicity assays, HEK293T cells were co-incubated with 50 μM derivative **6a**, and cell viability measured after 24 h by measuring conversion of resazurin to resuforin. For each assay, cells were trypsinized and seeded at 20 000 cells per well in a flat-bottom 96-well optical plate. Cells were seeded and incubated in full media (Dulbecco's Modified Eagle's Medium supplemented with 10% fetal bovine serum) containing 50 μM derivative **6a** and 1% DMSO. Vehicle control cells were incubated in full media with 1% DMSO only. After seeding into the optical plate, cells were incubated at 37 °C and 100% humidity with 5% atmospheric CO_2 for 20 h. Then, a resazurin solution in sterile PBS was added to each well to a final concentration of 25 μg mL^{-1}, after which cells were incubated for further 4 h. Well fluorescence was then measured at 590 nm emission and 560 nm excitation using a BioTek Synergy Hybrid plate reader. For the negative control, resazurin solution was added to full media alone and incubated for 4 h before measuring fluorescence. For data analysis, all values were normalized to vehicle control values. All measurements were made in triplicate.

For cell imaging experiments, images were obtained with a Leica DMi8 confocal microscope at 405 nm excitation, with emission filters of 420 ± 30 nm and 545 ± 30 nm for derivative **6a** and DCB, respectively. Prior to imaging, HEK293T cells were incubated with 10 μM derivative **6a** and 50 μM DCB for 16 h. For modified (pulse-chase) assays, DCB was removed after 12 h by washing cells once with full-serum media (DMEM + FBS), then fresh DMEM + FBS with 10 μM **6a** was added, and cells were incubated for further 4 h. Prior to imaging, all samples were washed once with DMEM + FBS, after which cells were incubated in DMEM + FBS only. Cells were imaged live at 37 °C and 100% humidity with 5% atmospheric CO_2. Image analysis was performed with the LAS X Life Science platform.

Conflicts of interest

The authors declare that there are no conflicts of interest in this work.

Acknowledgements

The authors thank CONACYT of Mexico for the financial support *via* project CB-2015/256359. A. S. O. V. and E. H. F. also thank CONACYT for scholarships 463817 (PhD) and 472413 (sabbatical), respectively. S. G. acknowledges support as a Beckman Scholar from the Arnold and Mabel Beckman Foundation.

References

1 A. Szłapa, S. Kula, U. Błaszkiewicz, M. Grucela, E. Schab-Balcerzak and M. Filapek, *Dyes Pigm.*, 2016, **129**, 80–89.

2 H. Xu, F. Wang, K. Wang, Y. Miao, J. Li, J. Zhang, H. Wang, Y. Hao and B. Xu, *Dyes Pigm.*, 2018, **155**, 84–92.
3 N. T. Kalyani and S. J. Dhoble, *Renewable Sustainable Energy Rev.*, 2012, **16**, 2696–2723.
4 C. Istanbulluoglu, S. Göker, G. Hizalan, S. O. Hacioglu, Y. A. Udum, E. D. Yildiz, A. Cirpan and L. Toppare, *New J. Chem.*, 2015, **39**, 6623–6630.
5 M. L. Keshtov, S. A. Kuklin, A. R. Khokhlov, I. O. Konstantinov, N. V. Nekrasova, Z. Xie and G. D. Sharma, *Polymer*, 2017, **133**, 195–204.
6 F. Silvestri, A. Marrocchi, M. Seri, C. Kim, T. J. Marks, A. Facchetti and A. Taticchi, *J. Am. Chem. Soc.*, 2010, **132**, 6108–6123.
7 Y. Zou, W. Wu, G. Sang, Y. Yang, Y. Liu and Y. Li, *Macromolecules*, 2007, **40**, 7231–7237.
8 Z. Liu, Z. Yang, T. Li, B. Wang, Y. Li, D. Qin, M. Wang and M. Yan, *Dalton Trans.*, 2011, **40**, 9370–9373.
9 K. Suzuki and T. Nagai, *Curr. Opin. Biotechnol.*, 2017, **48**, 135–141.
10 A. Miyawaki, *Nat. Rev. Mol. Cell Biol.*, 2011, **12**, 656–668.
11 J. T. Hou, W. X. Ren, K. Li, J. Seo, A. Sharma, X. Q. Yu and J. S. Kim, *Chem. Soc. Rev.*, 2017, **46**, 2076–2090.
12 Z. Guo, S. Park, J. Yoon and I. Shin, *Chem. Soc. Rev.*, 2014, **43**, 16–29.
13 Y. Chen, C. Zhu, Z. Yang, J. Chen, Y. He, Y. Jiao, W. He, L. Qiu, J. Cen and Z. Guo, *Angew. Chem., Int. Ed.*, 2013, **52**, 1688–1691.
14 T. Terai and T. Nagano, *Pflugers Arch.*, 2013, **465**, 347–359.
15 T. Nagano, *Proc. Jpn. Acad., Ser. B*, 2010, **86**, 837–847.
16 H. Zhang, R. R. Uselman and D. Yee, *Expert Opin. Med. Diagn.*, 2011, **5**, 241–251.
17 V. I. Martynov, A. A. Pakhomov, N. V. Popova, I. E. Deyev and A. G. Petrenko, *Acta Naturae*, 2016, **8**, 33–46.
18 E. Kim, Y. Lee, S. Lee and S. B. Park, *Acc. Chem. Res.*, 2015, **48**, 538–547.
19 J. C. Stockert and A. Blázquez-Castro, *Fluorescence Microscopy in Life Sciences*, Bentham Science Publishers, Glasgow, Scotland, 2017.
20 A. R. Katritzky and J.-C. M. Monbaliu, *The Chemistry of Benzotriazole Derivatives: A Tribute to Alan Roy Katritzky*, Springer International Publishing Switzerland, Liege, Belgium, 2016, vol. 43.
21 V. K. Singh, P. Rishishwar, P. Bhardwaj and S. Alok, *Int. J. Pharma Sci. Res.*, 2017, **8**, 446–456.
22 I. Briguglio, S. Piras, P. Corona, E. Gavini, M. Nieddu, G. Boatto and A. Carta, *Eur. J. Med. Chem.*, 2015, **97**, 612–648.
23 B. V. Suma, N. N. Natesh, C. H. S. Venkataramana, J. Jays and V. Madhavan, *Int. J. Pharm. Pharm. Sci.*, 2012, **4**, 169–173.
24 P. P. Dixit, V. J. Patil, P. S. Nair, S. Jain, N. Sinha and S. K. Arora, *Eur. J. Med. Chem.*, 2006, **41**, 423–428.
25 N. D. Gaikwad, S. V. Patil and V. D. Bobade, *Bioorg. Med. Chem. Lett.*, 2012, **22**, 3449–3454.
26 R. Loddo, F. Novelli, A. Sparatore, B. Tasso, M. Tonelli, V. Boido, F. Sparatore, G. Collu, I. Delogu, G. Giliberti and P. La Colla, *Bioorg. Med. Chem.*, 2015, **23**, 7024–7034.
27 C. M. Jamkhandi, J. I. Disouza, S. B. Magdum, K. B. Swami and P. S. Kumbhar, *Eur. J. Pharm. Med. Res.*, 2015, **2**, 302–306.
28 M. D. Dhanaraju, C. Gopi and V. G. Sastry, *Asian J. Res. Chem.*, 2015, **8**, 1–6.
29 J. Fu, Y. Yang, X.-W. Zhang, W.-J. Mao, Z.-M. Zhang and H.-L. Zhu, *Bioorg. Med. Chem.*, 2010, **18**, 8457–8462.
30 Y.-H. Yuan, M.-Z. Tian, J.-L. Wang, H. Xie, J. Qin and F. Feng, *RSC Adv.*, 2015, **5**, 69453–69457.
31 R. Gompper, P. Walther, C. Bräuchle and S. Stadler, *Tetrahedron*, 1996, **52**, 14607–14624.
32 B. M. Trost and X. Luan, *Nat. Protoc.*, 2012, **7**, 1497–1501.
33 O. Doebner, *Ber. Dtsch. Bot. Ges.*, 1900, **33**, 2140–2142.
34 E. Knoevenagel, *Chem. Ber.*, 1894, **27**, 2345–2346.
35 A. C. Borin, L. Serrano-Andrés, V. Ludwig and S. Canuto, *Phys. Chem. Chem. Phys.*, 2003, **5**, 5001–5009.
36 C. Sease, *Stud. Conserv.*, 1978, **23**, 76–85.
37 I. Novak, T. Abu-izneid, B. Kovač and L. Klasinc, *J. Phys. Chem. A*, 2009, **113**, 9751–9756.
38 I. Alkorta, G. Sánchez-Sanz, C. Trujillo, J. Elguero and R. M. Claramunt, *ARKIVOC*, 2012, **2012**, 85–106.
39 E. Hernández-Fernández, P. P. Sánchez-Lara, M. Ordóñez, O. A. Ramírez-Marroquín, F. G. Avalos-Alanís, S. López-Cortina, V. M. Jiménez-Pérez and T. R. Ibarra-Rivera, *Tetrahedron: Asymmetry*, 2015, **26**, 73–78.
40 F. Avalos-Alanis, E. Hernandez-Fernandez, P. Carranza-Rosales, S. Lopez-Cortina, J. Hernández-Fernández, M. Ordoñez, N. Guzman-Delgado, A. Morales-Vargas, V. Velázquez-Moreno and M. Santiago-Mauricio, *Bioorg. Med. Chem. Lett.*, 2017, **27**, 821–825.
41 O. A. Kucherak, P. Didier, Y. Mély and A. S. Klymchenko, *J. Phys. Chem. Lett.*, 2010, **1**, 616–620.
42 R. Ziessel, G. Ulrich and A. Harriman, *New J. Chem.*, 2007, **31**, 496–501.
43 B. Valeur and M. N. Berberan-Santos, *Molecular Fluorescence: Principles and Applications*, Wiley-VCH Verlag GmbH & Co. KGaA, Weinheim, Germany, 2nd edn, 2012.
44 R. Alford, H. M. Simpson, J. Duberman, G. C. Hill, M. Ogawa, C. Regino, H. Kobayashi and P. L. Choyke, *Mol. Imaging*, 2009, **8**, 341–354.
45 B. Herman, *Curr. Protoc. Cell Biol.*, 1998, **00**, A.1E.1–A.1E.5.
46 W. I. Lencer, P. Weyer, A. S. Verkman, D. A. Ausiello and D. Brown, *Am. J. Physiol.*, 1990, **258**, C309–C317.
47 G. Baravalle, D. Schober, M. Huber, N. Bayer, R. F. Murphy and R. Fuchs, *Cell Tissue Res.*, 2005, **320**, 99–113.
48 (*a*) Z. Liu and Y. Tu, *Synth. React. Inorg. Met.-Org. Chem.*, 2002, **32**, 265–276; (*b*) O. M. Ali, A. E. G. E. Amr and E. E. Mostafa, *Res. Chem. Intermed.*, 2013, **40**, 1545–1556; (*c*) N. I. Taha, *Int. J. Org. Chem.*, 2017, **07**, 219–228.
49 G. M. Sheldrick, *Acta Crystallogr., Sect. A: Found. Adv.*, 2015, **A71**, 3–8.
50 G. M. Sheldrick, *Acta Crystallogr., Sect. C: Struct. Chem.*, 2015, **C71**, 3–8.
51 P. Müller, *Crystallogr. Rev.*, 2009, **15**, 57–83.